Supporting Information

Probing Photocurrent Nonuniformities in the Subcells of Monolithic Perovskite/Silicon Tandem Solar Cells

Zhaoning Song[†], Jérémie Werner[‡], Niraj Shrestha[†], Florent Sahli[‡], Stefaan De Wolf[‡a)], Björn Niesen[‡§], Suneth C. Watthage[†], Adam B. Phillips[†], Christophe Ballif[‡§], Randy J. Ellingson[†] and Michael J. Heben[*†]*

† University of Toledo, Wright Center for Photovoltaics Innovation and Commercialization, Department of Physics and Astronomy, 2801 W. Bancroft St., Toledo, OH, 43606 USA.

‡ Ecole Polytechnique Fédérale de Lausanne (EPFL), Institute of Microengineering (IMT), Photovoltaics and Thin-Film Electronics Laboratory (PV-Lab), Rue de la Maladière 71b, 2002 Neuchâtel, Switzerland.

[a)] Now at King Abdullah University of Science and Technology (KAUST), KAUST Solar Center (KSC), Thuwal, 23955-6900, Saudi Arabia.

§ CSEM, PV-Center, Jaquet-Droz 1, 2002 Neuchâtel, Switzerland.

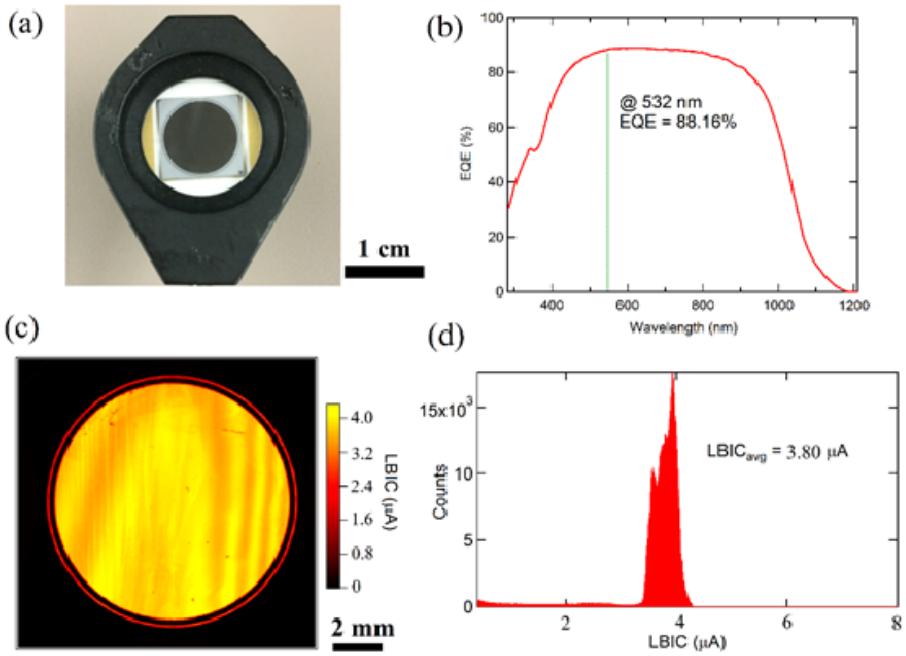

$$EQE = \frac{\#\ of\ collected\ charges}{\#\ of\ incident\ photons} = \frac{I}{I_{Si}} EQE_{Si}$$

Figure S1. (a) Optical image, (b) EQE, (c) LBIC map, and (d) LBIC histogram of the reference Si photodiode (Model: S2281-8D083, calibrated by NIST). The LBIC data for the perovskite/Si tandem devices was converted to EQE data using the equation above.

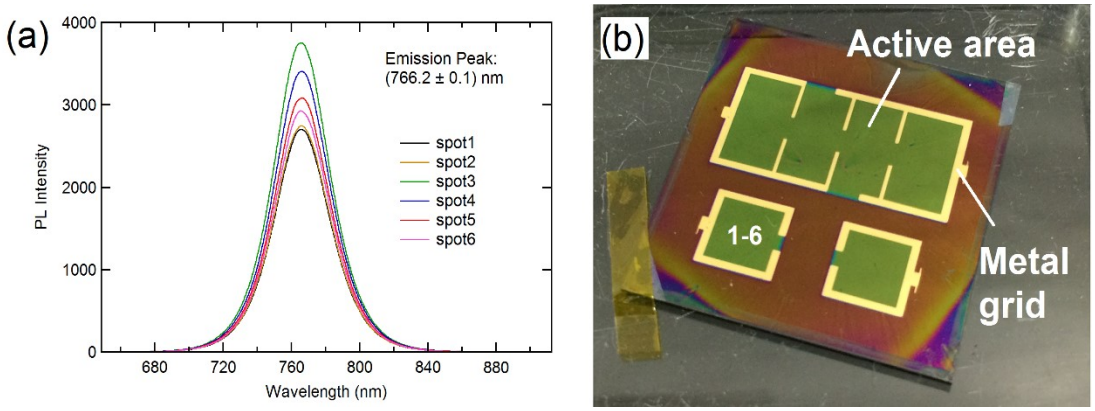

Figure S2. (a) Room temperature PL spectra of perovskite tandem cell measured in air at its various spots before LBIC measurement. (b) Photo of perovskite tandem cells.

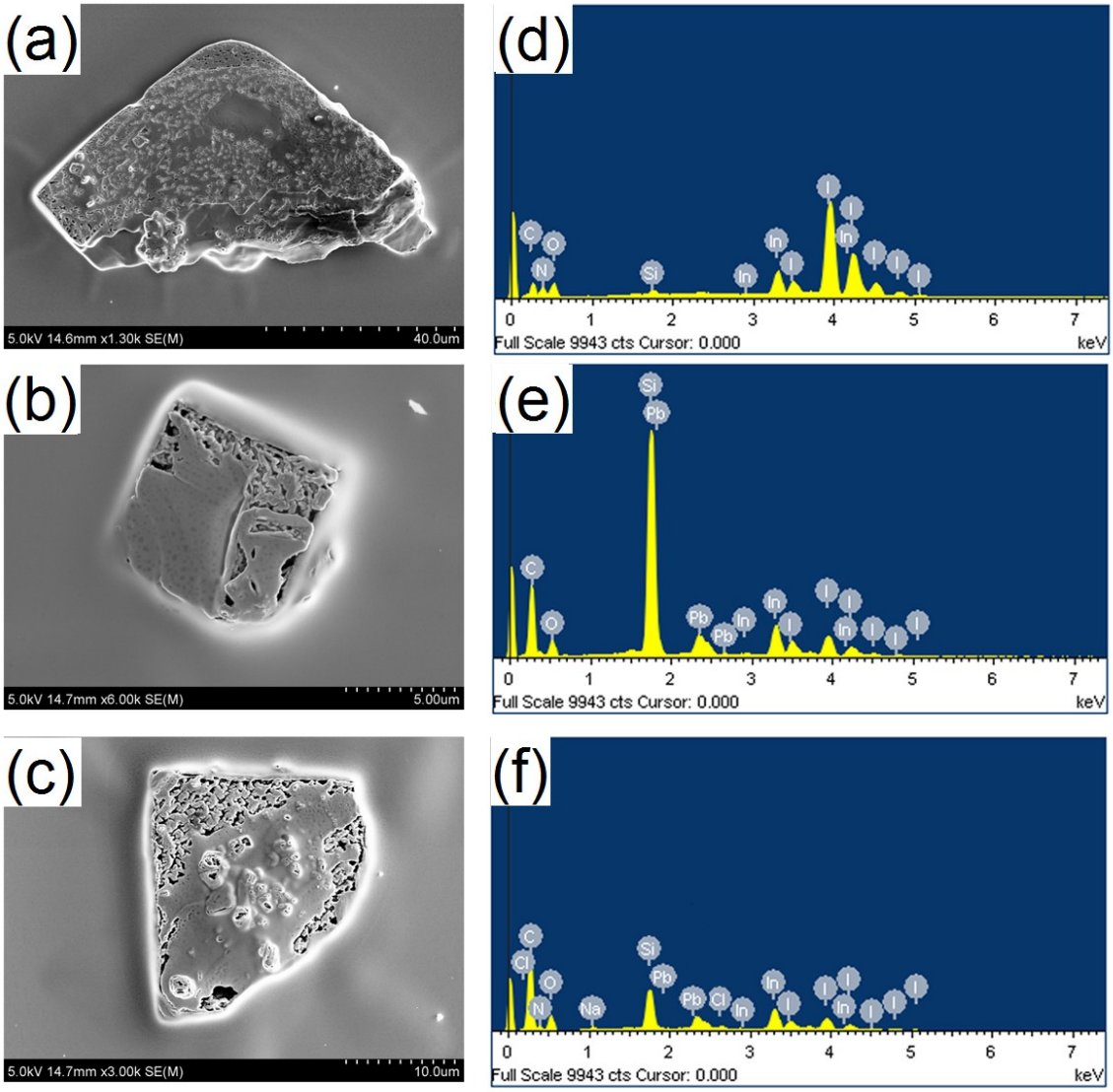

Figure S3. Electron microscopic image (a-c) and corresponding energy dispersive x-ray spectra (e-f) of three processing defects possibly caused by different spin processes. The image/spectrum that shows low concentrations of Pb and Si (a, d) could be associated with a large particle introduce by the PCBM/PEIE solutions that blocks the light. The defect without N (b, e) indicates the absence of spiro-OMeTAD. The defect with low I content (c, f) is likely associated with a deficiency of MAI or decomposition of the perovskite.

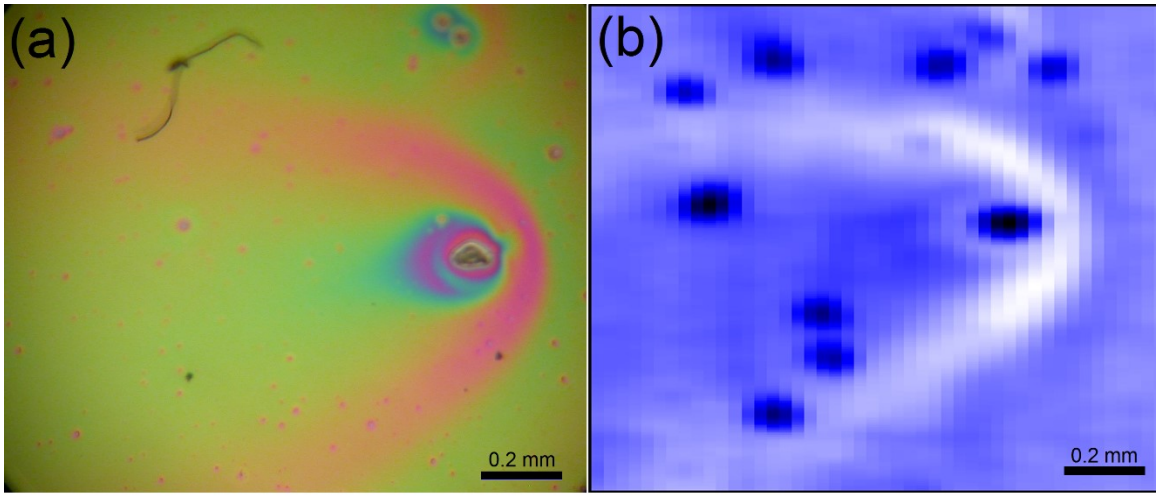

Figure S4. (a) Optical microscopic and (b) LBIC images of defects in the perovskite subcell. The pink comet streak indicates reduced green light reflection due changes in interference effects. These defects are most likely due to the spinning of Spiro-OMeTAD.

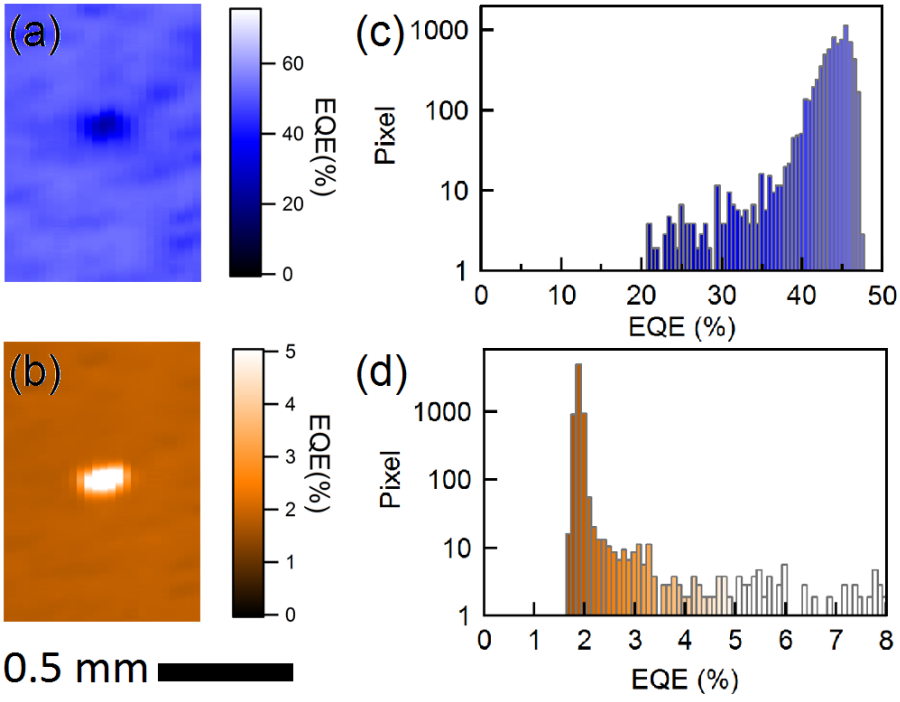

Figure S5. LBIC maps of the top (a) and bottom (b) cells of a typical defect in a perovskite/silicon tandem cell probed with the 532 nm laser under red or blue light-bias, respectively. Histograms of photocurrent distribution show different behaviors for the top (c) and bottom (d) cells.

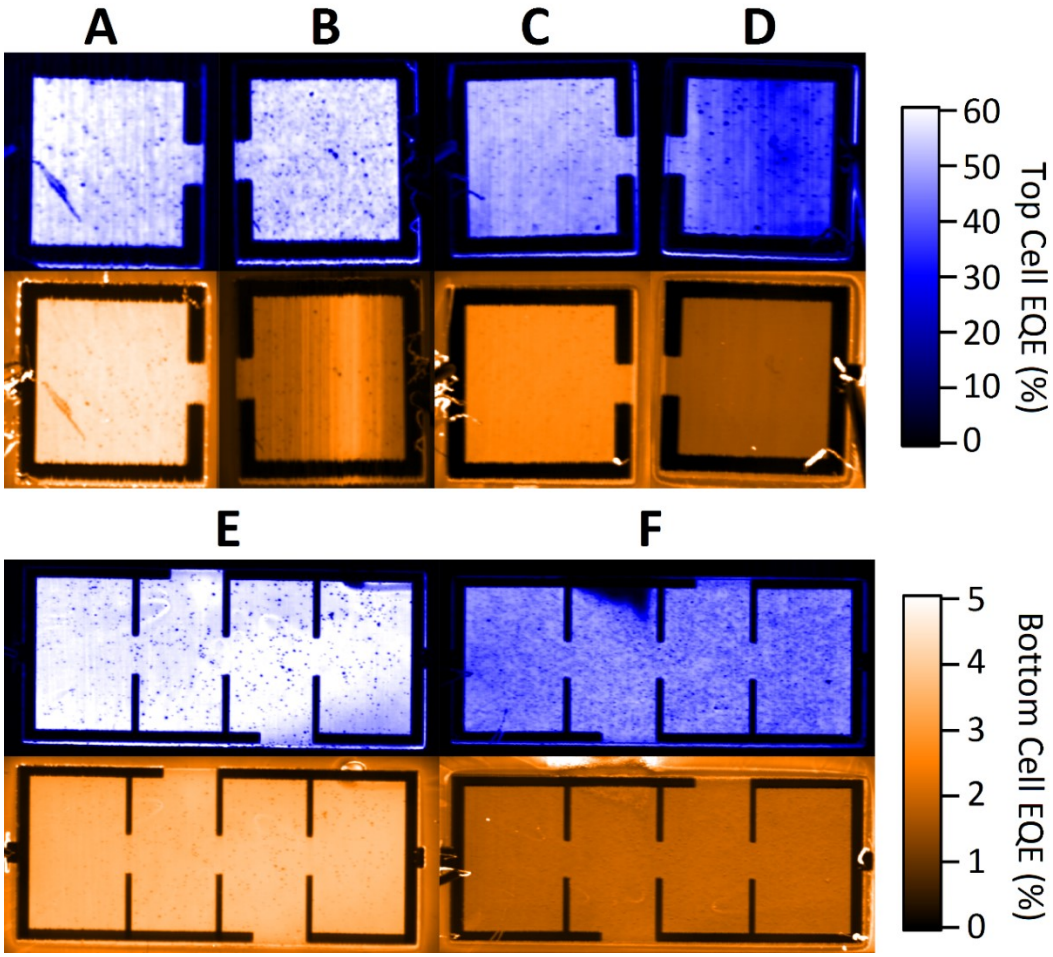

Figure S6. LBIC maps of top/bottom cells of 6 perovskite/Si tandem devices probed using the 532 nm laser. Note that the response varies in different devices.

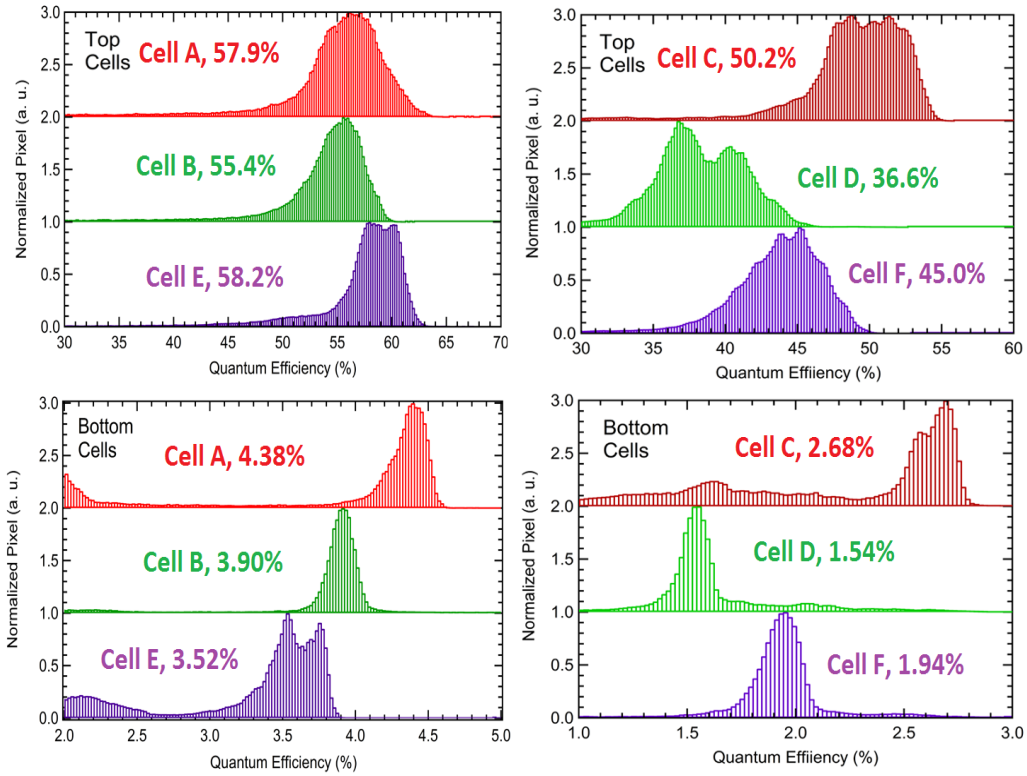

Figure S7. Histograms of the LBIC quantum efficiency distribution of the top and bottom cells of perovskite/Si devices measured using the 532 nm laser.

Quantifying the potential current improvement

The spatially averaged values of EQE determined by LBIC over the active area within the grid for the top/bottom cells (Figures 2a and 2b), 58.9% and 3.5%, respectively, are close to the large area, conventionally determined values at 532 nm (59.2% and 1.3%, respectively, as presented in Figure 1b). The higher value determined by LBIC would be expected if the perovskite cell's response were not completely saturated by the bias light. The LBIC intensity of ~8 suns was selected to avoid damage to the materials while still maintaining a good signal to background noise ratio (~100:1).

If the processing methods for the top cell can be improved, the uniformity of the current generation can be narrowed to the high end and the short circuit current of the devices can be improved. For instance, considering Cell E in Figure S4. If the current distribution under the lower peaks can be redistributed to the highest current peak, the quantum efficiencies would improve from 58.2% to 61.3% for the top cells and from 3.52% to 3.78% for the bottom cells. This would lead to a 5 to 15% improvement of J_{SC} in the top and bottom cells (up to ~3 mA/cm^2), assuming the whole EQE just scaling up as the improvement at 532 nm.

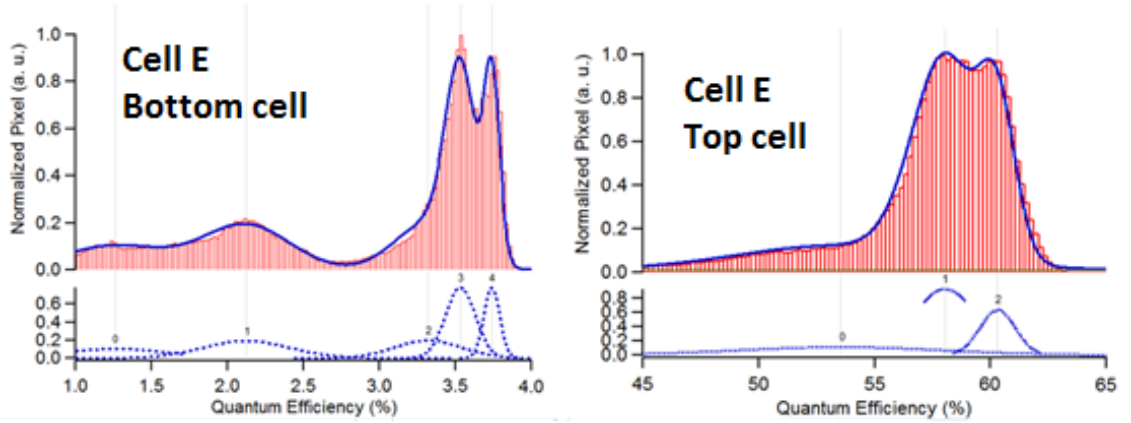

Figure S8. LBIC distribution analysis of Cell E.

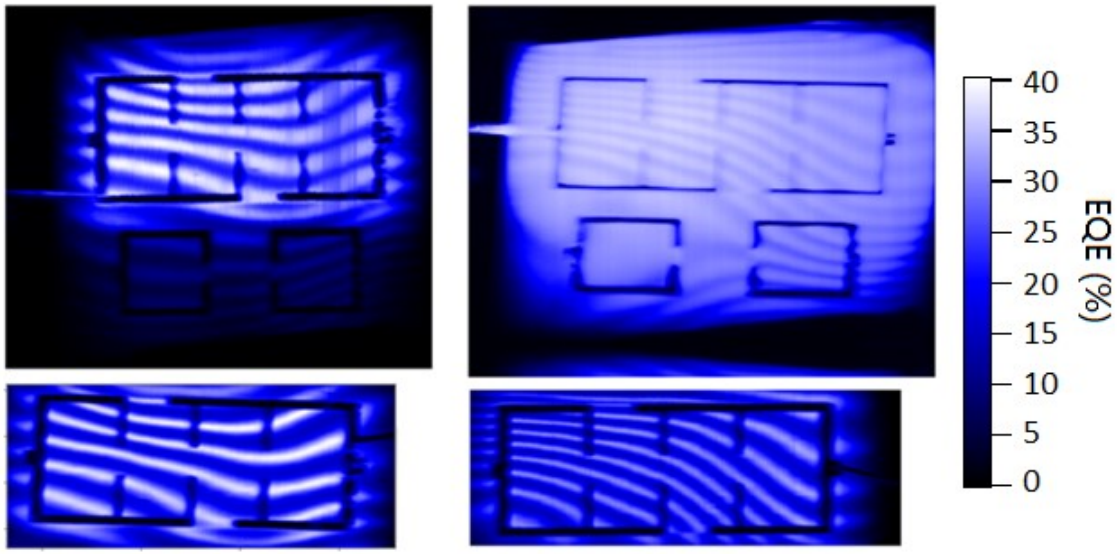

Figure S9. LBIC maps of silicon bottom cells in perovskite/Si tandem measured by the 1064 nm laser. The bottom images were maps after rotate the device at 90 and 180°.

Interference path length calculation.

Regarding the interference fringes, the light path difference between two fringes (bright & dark) can be express as 2*n*d* Cos (Theta) = m * L, where n is refractive index, d is the film thickness, Theta is the incident angle, m is an integer, and L is light wavelength. The basic (normal incidence) premise is that constructive interference will occur when the optical path length (2*n*d) satisfies 2nd = mL, so that the change in optical path length between adjacent maxima (or minima) is D = L/2n (for m = 1). If the interference fringes do arise from the Si, then m = ~4 (because the back surface is highly reflective Ag coating), L = 1064 nm (laser wavelength), n = 3.5 (Si refractive index), the thickness of the wafer change is D $\approx$ 4L/2n $\approx$ 600 nm.

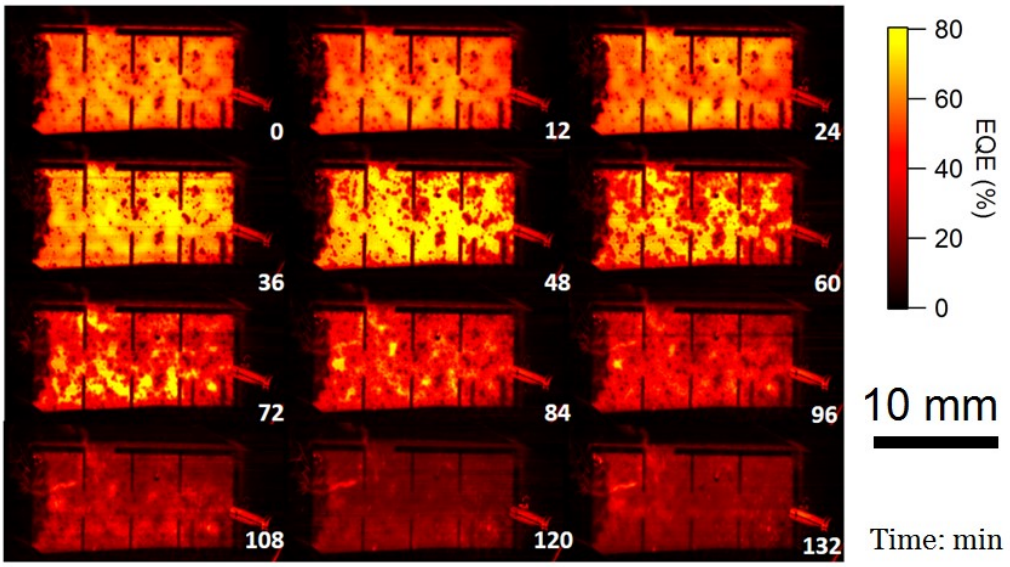

Figure S10. Degradation of the perovskite top cell in a perovskite/Si tandem under 80% relative humidity and red light bias. It can be noticed that the degradation of the top cell in the tandem is faster than that in the single junction perovskite cell, which is likely due to the photocatalytic reactions accelerated by the infrared light bias.

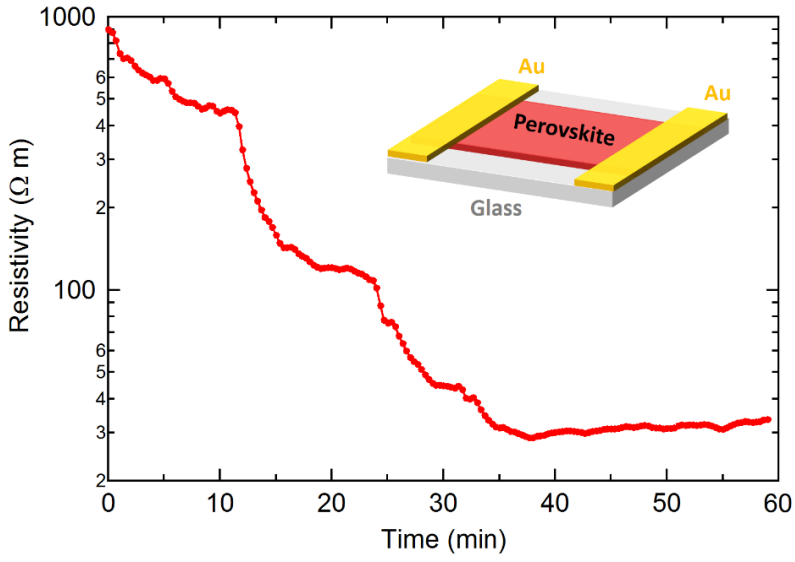

Figure S11. Evolution of resistivity of a perovskite film deposited on a glass substrate after exposure to moisture of 80% relative humidity. The resistivity was calculated from a series of I-V curves measured at a 20 s interval.

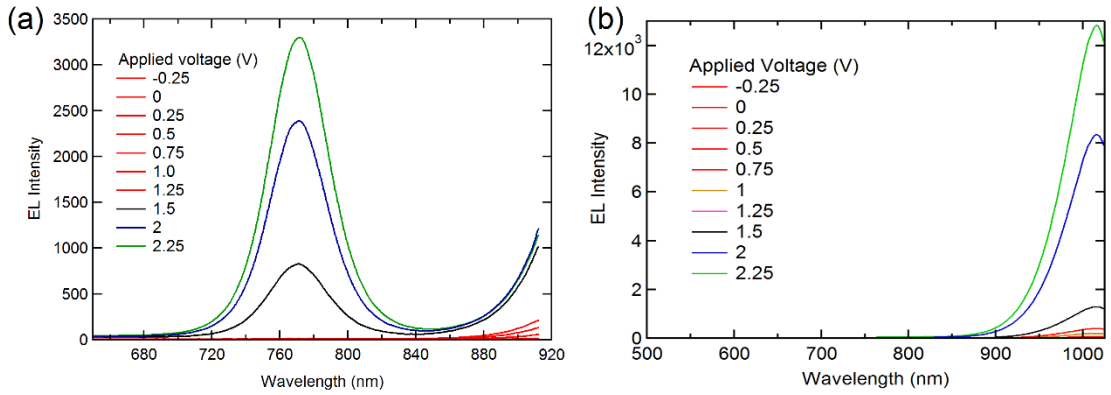

Figure S12. EL spectra of a perovskite/Si tandem solar cell (a) before and (b) after degradation test.